

Retinal Ganglion Cell Dysfunction in Asymptomatic G11778A: Leber Hereditary Optic Neuropathy

John Guy, William J. Feuer, Vittorio Porciatti, Joyce Schiffman, Fawzi Abukhalil, Ruth Vandenbroucke, Potyra R. Rosa, and Byron L. Lam

Bascom Palmer Eye Institute University of Miami, Miller School of Medicine, Miami, Florida

Correspondence: John Guy, Bascom Palmer Eye Institute, McKnight Building Room 404, 1638 NW 10th Avenue, Miami, FL 33136; jguy@med.miami.edu.

Submitted: September 30, 2013
Accepted: December 9, 2013

Guy G, Feuer WJ, Porciatti V, et al. Retinal ganglion cell dysfunction in asymptomatic G11778A: Leber hereditary optic neuropathy. *Invest Ophthalmol Vis Sci.* 2014;55:841-848. DOI:10.1167/iovs.13-13365

PURPOSE. To report the serial evaluation of asymptomatic eyes of subjects with mutated G11778A mitochondrial DNA.

METHODS. Forty-five asymptomatic G11778A Leber hereditary optic neuropathy (LHON) carriers and two patients with the mutation who developed unilateral visual loss underwent testing that included visual acuity, automated visual field, pattern electroretinogram (PERG), and spectral-domain optical coherence tomography every 6 months between September 2008 and March 2012.

RESULTS. Visual acuity, visual fields, and retinal nerve fiber layer thickness remained stable within the normal range. Mean PERG amplitudes of carriers dropped progressively by ~40% from baseline to 36 months. In addition, comparisons with the fellow eyes of patients with unilateral optic neuritis revealed a 3.4 ETDRS (Early Treatment Diabetic Retinopathy Study) letter loss in the LHON carriers. A single carrier developed visual loss, with PERG amplitudes dropping by half. In one of two LHON cases who presented with unilateral visual loss, visual acuity in the asymptomatic eye was ~20/40 at baseline. The PERG amplitude of this eye was reduced to ~30% of normal. Six months later, his visual acuity had dropped to ~20/500. A second patient who was ~20/20 and had a visual field defect in the asymptomatic eye at baseline remained at this level for the 18 months of follow-up. His PERG amplitudes were similar to those of asymptomatic carriers, with 0.78 μ V at baseline that did not decline with follow-up.

CONCLUSIONS. Declines of the PERG amplitude suggest subclinical retinal ganglion cell dysfunction in asymptomatic G11778A subjects, which is progressive.

Keywords: Leber hereditary optic neuropathy, electrophysiology, mitochondrial DNA

Leber hereditary optic neuropathy (LHON) is a maternally inherited mitochondrial genetic disease characterized by severe visual loss.¹ The clinical findings were first described in 1871 by Theodore Leber.² LHON typically occurs in later childhood and early adulthood with little or no propensity for recovery.³ Affected individuals are usually entirely asymptomatic until they develop visual blurring affecting the central visual field.⁴ Onset of visual loss initially may be simultaneous in both eyes or in just one eye.⁵ If unilateral, similar symptoms typically appear in the other eye within 2 months and, in fact, such patients have been shown to have subtle defects on automated perimetry in the asymptomatic eye before that eye's visual decline.⁶

The association of LHON with the G11778A mutation in mitochondrial DNA (mtDNA) was first described by Wallace and coworkers⁷ in 1988. Approximately half the men and approximately 10% of women who have mutated G11778A mtDNA will eventually lose vision. No testing is capable of predicting who will develop the phenotype⁸⁻¹⁰ and currently, available therapies are either ineffective or not robust.^{6,11-15}

Analysis of baseline entry data of our first year of recruitment (25 affected and 21 carriers) into the study was described in 2010.¹⁶ In that study four asymptomatic carriers have pattern electroretinogram (PERG) amplitudes that are less than 75% of normal. They have no abnormalities detected on

clinical examination or structure changes of the retinal nerve fiber layer (RNFL) on optical coherence tomography (OCT). Since the PERG is a sensitive measure of retinal ganglion cell (RGC) function, we hypothesized that it may be useful in detecting subclinical disease¹⁷ that later evolves into the LHON phenotype. The current report focuses on the serial evaluation of the asymptomatic eyes of these and additional subjects with mutated G11778A mtDNA. Here we show that progressive declines in the PERG identify early RGC dysfunction in asymptomatic eyes.

METHODS

Clinical

Maternally related family members of G11778A LHON patients were recruited at the Bascom Palmer Eye Institute by two neuro-ophthalmologists (JG and BLL) and re-examined every 6 months. Informed consent, approved by the University of Miami Institutional Review Board, was obtained from LHON patients and their maternally related family members at their baseline visit. Best-corrected visual acuity was measured by using the Early Treatment Diabetic Retinopathy Study (ETDRS) chart every 6 months. Neuro-ophthalmic examination also included assessments of the pupils and anterior segment as well

as ophthalmoscopy of the optic nerve head and retina. Visual fields were obtained every 6 months with the Humphrey 30-2 white-on-white SITA-standard automated perimetry (Carl Zeiss Meditec, Dublin, CA). Cataracts, retinal or optic nerve diseases other than LHON were exclusion criteria. The visual function of asymptomatic LHON carriers was compared to the public database of asymptomatic eyes of patients with unilateral optic neuritis at baseline who were entered into the optic neuritis treatment trial. The study was conducted in compliance with the Declaration of Helsinki.

Molecular Analysis

Genomic DNA was obtained from each patient's white blood cells obtained from venous blood. A PCR-based test using the amplification refractory mutation system (ARMS) was used to detect the presence or absence of three nucleotide substitutions known to cause LHON (3460 G > A, 11778 G > A, or 14484 T > C). Two PCR cocktails, one with primers corresponding to the normal sequences and one with primers corresponding to the mutant sequences, were used to amplify patient DNA. Together, these amplifications revealed the normal and mutant genotypes. An additional primer pair, corresponding to a region of chromosome 7, was included in the mutant PCR cocktails as an internal amplification control. All positive ARMS results were confirmed with bidirectional DNA sequencing. Molecular analysis was performed by the Carver laboratory at the University of Iowa.¹⁸ Subjects were tested for heteroplasmy and secondary mutations in the *ND4* gene. Six of the carriers had molecular analysis that was performed by Athena Laboratories (Worcester, MA). Heteroplasmy and secondary mutations for these subjects were not reported by Athena.

Optical Coherence Tomography

Peripapillary RNFL thickness was measured by an Optic Disk Cube 200 × 200 scan of the spectral domain Cirrus HD OCT (software version 3.0; Carl Zeiss Meditec). Cirrus SD-OCT uses spectral-domain OCT (SD-OCT) technology to acquire data with high resolution (5 μm) and has a scanning rate of 27,000 A-scans per second. The Optic Disk Cube 200 × 200 protocol was used for acquisition and analysis. This protocol generates a cube of data through a 6-mm square grid by acquiring a series of 200 horizontal scan lines each composed of 200 A-scans. The total scan time was 1.48 seconds. For analysis, Cirrus algorithms identify the center of the optic disc and automatically place a calculation circle of 3.46-mm diameter around it. The anterior and posterior margins of the RNFL are delineated, and after extracting from the data cube 256 A-scan samples along the path of the calculation circle, the system calculates the RNFL thickness at each point on the circle. Three consecutive Optic Disk Cube scans were acquired and analyzed for each eye.¹⁹

Electrophysiology

The PERG was recorded simultaneously from both eyes according to a paradigm optimized for glaucoma detection (PERGLA)²⁰ (Fig. 1). The method is highly reproducible,²¹ and normative data are available.²² Details of the PERGLA protocol have previously been described.²⁰ In brief, retinal signals were recorded by means of skin electrodes taped on the lower eyelids (Fig. 1A). Subjects were fitted with the appropriate correction for their refractive error and were instructed to fixate on a target at the center of a pattern stimulus placed at a viewing distance of 30 cm. Subjects did not receive dilating drops and were allowed to blink freely. The pattern stimulus

consisted of horizontal gratings (1.7 cyc/deg, 25° diameter circular field, 98% contrast, 40 cd/m² mean luminance), reversing in counterphase at 8.14 Hz (16.28 reversals per second). The pattern stimulus (Fig. 1B) was generated on a cathode ray tube display (65-Hz refresh rate, not interlaced) placed at the bottom of a Ganzfeld bowl to minimize the influence of ambient room lighting. Electrical signals were band-pass filtered (1–30 Hz), amplified (100,000 fold), and averaged in synchrony with the reversal period. During signal acquisition, sweeps contaminated by eye blinks or gross eye movements were rejected automatically over a threshold voltage of 25 μV. Two successive responses of 300 artifact-free sweeps each were recorded, separated by a brief pause. The first 30 sweeps of each response were rejected to allow steady-state conditions. The software allowed visual inspection of the two consecutive responses superimposed to check for consistency and then computed the final PERG waveform (600 artifact-free sweeps). As the PERG was recorded in response to relatively fast alternating gratings, the response waveforms were typically sinusoidal-like, with a temporal period corresponding to the reversal rate. Pattern electroretinogram waveforms were automatically analyzed in the frequency domain by discrete Fourier transform to isolate the frequency component at the contrast-reversal rate (16.28 Hz) and compute its amplitude in microvolts and phase in π radians.

The standardized PERG recording protocol included a measure of within-test variability.^{23,24} Namely, for each measurement of each eye, two successive responses of 300 artifact-free sweeps each were recorded (Fig. 1C), separated by a brief pause. Pattern electroretinogram software allowed visual inspection of the two consecutive responses superimposed to check for consistency, and then computed the final PERG waveform (600 artifact-free sweeps) and the coefficient of variation (CV = standard deviation [SD]/mean expressed as %) of amplitude and phase of the two partial averages, which represents a measure of within-test variability. These CVs along with the amplitude and phase measurements for each measurement were used to calculate pooled test-retest standard deviations for the sample of carriers and, from these, intraclass correlation coefficients were calculated. Reliability data are presented for the right eye measurements at baseline and the 36-month visits.

Statistical Analysis

Values were expressed as means ± SD. Owing to the strong age dependency of the PERG, these measurements also were expressed as percentage of age-specific normal.²⁵ The effect of months followed on each dependent variable was assessed by including visit months as a linear covariate in a mixed-model analysis of variance along with subject as a random effect. A *P* value of < 0.05 was considered significant, and values < 0.01 were considered highly significant.

RESULTS

Forty-five unaffected G11778A LHON carriers, 6 (13%) males and 39 (87%) females, were recruited between September 2008 and March 2012 and returned for one or more follow-up visits (6 to 36 months) as of August 2012. All carriers were maternal relatives of affected LHON family members who were entered into the study. Mean age at the time of recruitment was 21.3 (SD = 10.4) years for males and 42.6 (SD = 18.1) years for females. LHON carriers were 100% homoplasmic for the G11778A mtDNA mutation with the exception of six female carriers who were 50% heteroplasmic (*n* = 3), 70% heteroplasmic (*n* = 2), or 80% heteroplasmic (*n* =

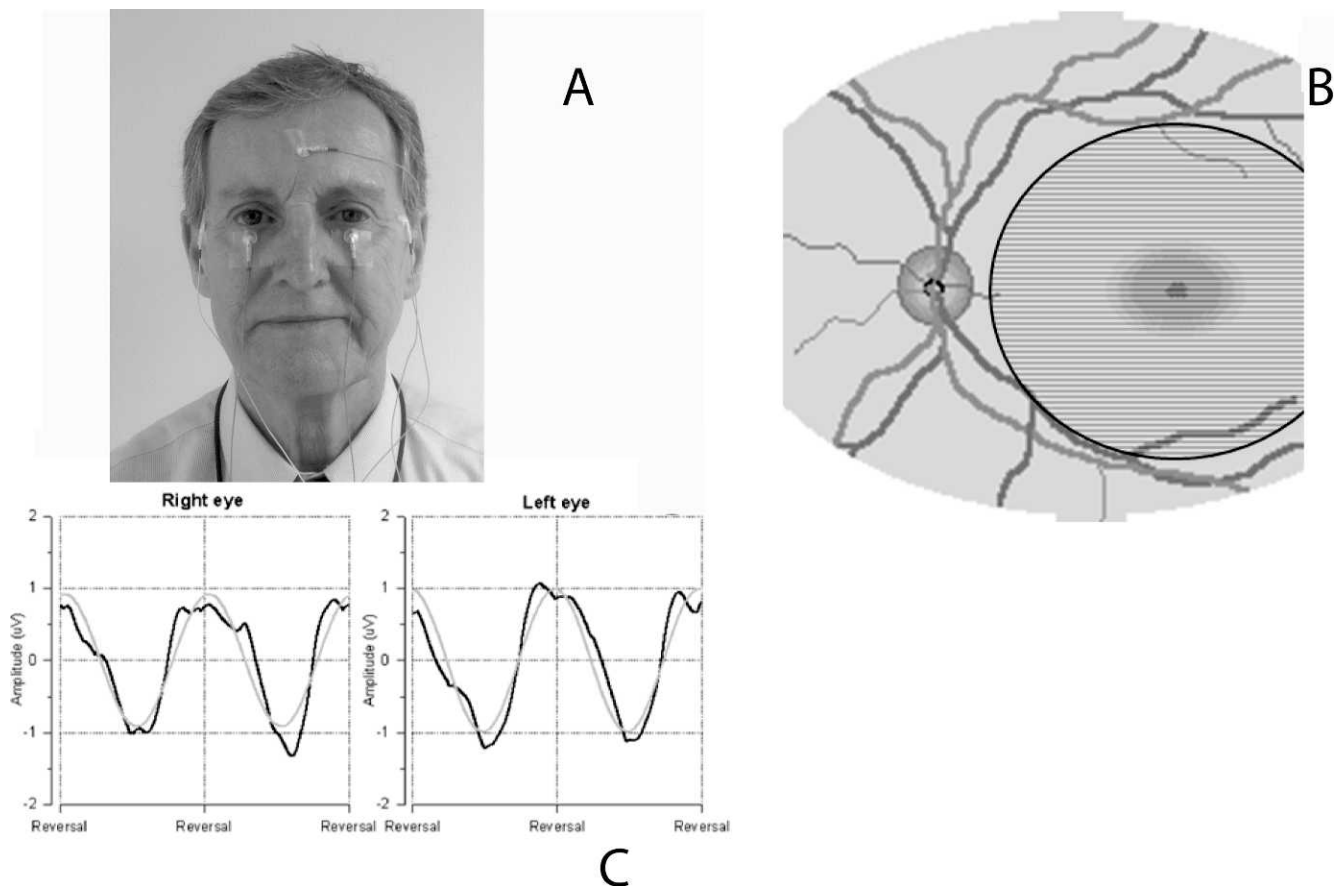


FIGURE 1. Illustration of the PERG setup shows that (A) surface electrodes are taped on the lower eyelids (active), temples (reference), and forehead (common ground). (B) The subject looks for 3 minutes at a stimulus consisting of horizontal black and white stripes alternating 16.6 times per second. The stimulus covers a circular retinal area with a 12.5° radius centered on the fovea. (C) Examples of normal PERG waveforms recorded simultaneously from both eyes (*black lines*: unprocessed PERG waveforms; *grey lines*: time-domain representations of 16.6-Hz response components isolated with discrete Fourier transform, from which PERG amplitude and phase are calculated).

1). Because the length of participation in this study varied from carrier to carrier, different subsets of subjects are included at each visit, and the baseline means, which include all participants, may not always be a representative comparison. Therefore, the demographics and means and SDs are provided in Table 1 and the changes over time with P values are provided in Table 2.

Visual Acuity

The asymptomatic G11778A LHON carriers had a mean visual acuity of 87.8 (SD = 3.8) ETDRS letters at baseline. Visual acuity did not diminish at 6 months (87.4 letters, SD = 4.0, $n = 44$), at 12 months (87.9 letters, SD = 3.5, $n = 38$), at 18 months (87.6 letters, SD = 4.5, $n = 35$), at 24 months (87.5 letters, SD = 3.7, $n = 23$), at 30 months (88.9 letters, SD = 4.4, $n = 21$), or at 36 months (87.1 letters, SD = 3.7, $n = 14$) of follow-up (Fig. 2). There was a slight, but statistically significant increase of 0.4 (SE = 0.2) letters read per 12 months of follow-up ($P = 0.022$), perhaps due to a learning effect.

When we compared the visual acuity of our asymptomatic subjects with mutated G11778A mt DNA to the visual acuity of the contralateral asymptomatic eyes of patients with acute unilateral optic neuritis who were entered into the Optic Neuritis Treatment Trial (ONTT),^{26,27} we found a 3.4 letter loss of visual acuity in the LHON carriers (Fig. 3). This difference was highly significant, $P = 0.001$. The ages of the groups also

were significantly different, but the lines relating ETDRS letters to age are roughly parallel, nearly flat, and of different heights, so age does not explain differences between ONTT fellow eyes and LHON carriers. This finding was confirmed by an analysis of covariance, $P = 0.001$. Thus, slight visual loss was detected in asymptomatic LHON subjects and it was worse than that of contralateral asymptomatic eyes of patients with acute unilateral optic neuritis.

Visual Fields

The visual field mean defect (MD) for asymptomatic carriers was -1.83 (SD = 1.66) dB at baseline, -1.59 (SD = 1.34) dB at 6 months, -1.48 (SD = 1.51) dB at 12 months, -1.72 (SD = 1.37) dB at 18 months, -1.64 (SD = 1.64) dB at 24 months, -1.76 (SD = 1.66) dB at 30 months, and -1.59 (SD = 1.47) dB at 36 months (Fig. 4). We found no statistically significant change in Humphrey visual field (HVF) MD over follow-up for asymptomatic G11778A carriers ($P = 0.49$). Looking for trends, we placed 95% confidence intervals around the nonsignificant slopes relating visual field MD to months of follow-up. If there is a decrease in HVF MD in LHON carriers, it is likely no more than -0.2 dB per year. Comparisons of baseline values of asymptomatic fellow eyes of ONTT patients (HVF MD = -3.14) revealed values that were almost double those of the baseline values for LHON carriers. Even after adjusting for age this difference was statistically significant ($P = 0.005$). Thus, visual

TABLE 1. Patient Characteristics and Visual Function Measurements by Follow-up Visit

| | Patient Characteristics at Enrollment for Those Followed at Each Study Visit | | | | | | | | | | | |
|---------------------------------|--|------------------|------------------|------------------|------------------|------------------|------------------|------------------|------------------|------------------|------------------|------------------|
| | Month 6, N = 45* | Month 12, N = 38 | Month 18, N = 32 | Month 24, N = 23 | Month 30, N = 21 | Month 36, N = 14 | Month 6, N = 45* | Month 12, N = 38 | Month 18, N = 32 | Month 24, N = 23 | Month 30, N = 21 | Month 36, N = 14 |
| Female sex, No. (%) | 39 (87) | 33 (87) | 27 (84) | 19 (83) | 18 (86) | 12 (86) | 39 (87) | 33 (87) | 27 (84) | 19 (83) | 18 (86) | 12 (86) |
| Age at enrollment, mean (SD), y | 42.6 (±18.1) | 43.3 (±18.3) | 45.3 (±16.6) | 45.0 (±17.4) | 45.8 (±17.5) | 50.3 (±16.1) | 42.6 (±18.1) | 43.3 (±18.3) | 45.3 (±16.6) | 45.0 (±17.4) | 45.8 (±17.5) | 50.3 (±16.1) |
| Male sex, No. (%) | 6 (13) | 5 (13) | 5 (16) | 4 (17) | 3 (14) | 2 (14) | 6 (13) | 5 (13) | 5 (16) | 4 (17) | 3 (14) | 2 (14) |
| Age at enrollment, mean (SD), y | 21.2 (±10.4) | 19.6 (±10.7) | 19.6 (±10.7) | 20.9 (±12.0) | 19.8 (±14.4) | 22.8 (±19.0) | 21.2 (±10.4) | 19.6 (±10.7) | 19.6 (±10.7) | 20.9 (±12.0) | 19.8 (±14.4) | 22.8 (±19.0) |

| | Mean (SD) Visual Function Measurements at Baseline and Follow-up for Those Followed Up at Each Study Visit | | | | | | | | | | | | | |
|--------------------|--|------------------|------------------|------------------|------------------|------------------|------------------|---------------|------------------|------------------|------------------|------------------|------------------|------------------|
| | Baseline | Month 6, N = 45* | Month 12, N = 38 | Month 18, N = 32 | Month 24, N = 23 | Month 30, N = 21 | Month 36, N = 14 | Baseline | Month 6, N = 45* | Month 12, N = 38 | Month 18, N = 32 | Month 24, N = 23 | Month 30, N = 21 | Month 36, N = 14 |
| ETDRS letters | 87.8 (±3.8) | 87.4 (±4.0) | 87.9 (±3.9) | 87.7 (±4.2) | 87.6 (±4.5) | 87.8 (±4.7) | 87.8 (±4.4) | 87.8 (±4.7) | 87.5 (±3.9) | 87.5 (±3.9) | 87.8 (±4.4) | 88.9 (±4.4) | 87.3 (±5.0) | 87.1 (±3.7) |
| HVF MD, dB | -1.85 (±1.66) | -1.59 (±1.36) | -1.74 (±1.77) | -1.67 (±1.78) | -1.71 (±1.39) | -1.74 (±2.06) | -1.71 (±1.64) | -1.71 (±1.64) | -1.64 (±1.64) | -1.64 (±1.64) | -1.71 (±1.64) | -1.76 (±1.66) | -1.86 (±2.11) | -1.59 (±1.47) |
| Average RNFL, μm | 96.9 (±11.6) | 97.8 (±12.6) | 95.9 (±11.5) | 94.0 (±11.4) | 94.6 (±11.8) | 91.1 (±10.9) | 90.8 (±11.1) | 91.2 (±11.4) | 90.8 (±11.1) | 90.8 (±11.1) | 91.2 (±11.4) | 91.6 (±11.1) | 90.5 (±13.2) | 91.7 (±13.6) |
| PERG amplitude, μV | 1.01 (±0.44) | 0.92 (±0.35) | 1.00 (±0.42) | 1.01 (±0.41) | 0.82 (±0.31) | 0.88 (±0.3) | 0.77 (±0.25) | 1.02 (±0.33) | 0.77 (±0.25) | 0.77 (±0.25) | 1.02 (±0.33) | 0.82 (±0.27) | 0.94 (±0.34) | 0.61 (±0.30) |
| PERG phase, π rad | 1.83 (±0.10) | 1.82 (±0.10) | 1.81 (±0.10) | 1.83 (±0.10) | 1.81 (±0.12) | 1.82 (±0.11) | 1.80 (±0.15) | 1.82 (±0.11) | 1.80 (±0.15) | 1.80 (±0.15) | 1.82 (±0.11) | 1.77 (±0.13) | 1.81 (±0.11) | 1.84 (±0.24) |

* All 45 carriers returned for the 6-month follow-up visit. F Up, follow-up.

field defects were worse in ONTT fellow eyes than in LHON carriers.

Optical Coherence Tomography

Seventeen (38%) of our carriers had RNFL values greater than 100 μm, suggesting presymptomatic thickening. Average RNFL thickness of our carriers was 96.4 (SD = 11.6) μm at baseline, 97.8 (SD = 12.6) μm at 6 months, 96.2 (SD = 12.3) μm at 12 months, 94.6 (SD = 11.8) μm at 18 months, 90.8 (SD = 11.0) μm at 24 months, 92.1 (SD = 11.1) μm at 30 months, and 91.7 (SD = 13.6) μm at 36 months (all $P > 0.20$) (Fig. 5). There was no statistically significant change in RNFL thickness over follow-up ($P = 0.19$). Looking for trends, we placed 95% confidence intervals around the nonsignificant slopes relating RNFL thickness to months of follow-up. If there is a decrease in RNFL thickness, it is likely no more than -0.2 μm per year. This extent of thinning is commensurate with the known effect of normal aging on RNFL thickness.²⁸

Pattern Electroretinogram

We observed a significant decrease in PERG amplitude measures in LHON carriers (Fig. 6A, 6B). Mean PERG amplitude dropped from 1.01 (SD = 0.44) μV at baseline to 0.92 (SD = 0.35) μV at 6 months, 0.83 (SD = 0.33) μV at 1 year, 0.82 (SD = 0.31) μV at 18 months, 0.77 (SD = 0.25) μV at 24 months, 0.82 (SD = 0.27) μV at 30 months, and 0.61 (SD = 0.30) μV at 36 months. There was a highly significant 0.084 (SE = 0.012) decrease in PERG amplitude per year of follow-up ($P < 0.001$). This decrease in PERG amplitude was not affected by adjusting for RNFL ($P < 0.001$). Losses were not associated with age or sex. Amplitude losses of 10% or more occurred in 51% of carriers by 6 months and in 61% of carriers by 12 months after enrollment. Mean PERG phase was 1.83 (SD = 0.10) π rad at baseline, 1.83 (SD = 0.10) π rad at 6 months, and 1.81 (SD = 0.09) π rad at 1 year, 1.81 (SD = 0.12) π rad at 18 months, 1.80 (SD = 0.15) π rad at 2 years, 1.77 (SD = 0.13) π rad at 30 months, and 1.84 (SD = 0.24) π rad at 3 years (Fig. 6C). There was no statistically significant change in PERG phase over follow-up ($P = 0.22$).

The average (SD) of right eye coefficients of variation for PERG amplitude and phase at baseline were 15.3% (12.9) and 1.6% (1.3), respectively, similar to those of normal control patients from a previous study conducted by our group, 2.3% (7.8) and 1.1% (0.8), respectively.²⁹ At 36 months, carrier average amplitude CVs increased to 18.1% (15.7) but not significantly so ($P = 0.062$, paired t -test). This was also true of average phase CV, 2.2% (2.0) ($P = 0.081$, paired t -test). Pooled baseline test-retest SDs for amplitude and phase were, respectively, 0.15 μV and 0.13 π rad. Intraclass correlation coefficients for amplitude and phase at baseline and 36 months ranged from 0.87 to 0.94, which are in the range usually considered excellent.³⁰

Conversion to Affected

The 19-year-old brother of an LHON-affected patient was first examined in November 2010. At baseline, his ETDRS acuity was 88 letters OD and 90 letters OS. Visual fields were normal with MD = -0.43 dB OD and -1.11 dB OS. The optic nerve heads showed no swelling or pallor. Mean RNFL thickness was 107 μm OD and 107 μm OS. PERG amplitudes were 1.25 μV OD and 1.00 μV OS. Pattern electroretinogram phase was 1.87 π rad OD and 1.89 π rad OS. In January 2013, outside reports showed his visual acuity had dropped to 20/60 in the right eye and 20/80 in the left eye. Visual fields now showed small central scotomas with MD = -1.48 dB OD and -1.69 dB OS. In

TABLE 2. Mean (SD) Follow-up Minus Baseline Changes for Each Measured Parameter

| | Month 6 | Month 12 | Month 18 | Month 24 | Month 30 | Month 36 | P Value* |
|-------------------------------|--------------|--------------|--------------|--------------|--------------|--------------|----------|
| ETDRS letters | -0.43 (2.84) | -0.01 (2.61) | -0.06 (3.36) | -0.3 (3.49) | 1.07 (3.25) | -0.14 (3.95) | 0.022 |
| HVF MD, dB | 0.24 (1.19) | 0.26 (1.47) | -0.04 (1.45) | 0.11 (1.9) | -0.04 (1.85) | 0.28 (1.9) | 0.49 |
| Average RNFL, μm | 0.87 (4.53) | 0.29 (4.43) | 0.53 (3.41) | -0.33 (3.07) | 0.40 (3.73) | 1.18 (3.33) | 0.19 |
| PERG amplitude, μV | -0.09 (0.31) | -0.17 (0.25) | -0.19 (0.29) | -0.11 (0.25) | -0.2 (0.28) | -0.32 (0.26) | <0.001 |
| PERG phase, $\xi \pi$ rad | -0.01 (0.04) | -0.02 (0.06) | -0.02 (0.09) | -0.02 (0.1) | -0.05 (0.07) | 0.03 (0.2) | 0.22 |

* Mixed.

April 2013, on presentation to our unit, ETDRS visual acuity dropped to 15 letters OD and 19 letters OS. Visual fields now showed dense central scotomas with MD = -15.70 dB OD and -19.1 dB OS. Ophthalmoscopy revealed temporal pallor of both optic nerves. Optical coherence tomography showed thickening of the RNFL with average values of 119 μm OD and 114 μm OS. Pattern electroretinograms had dropped to 0.57 μV OD and 0.55 μV OS, and phase was delayed to 1.98 π rad OD and 2.01 π rad OS.

PERG Amplitudes in the Fellow Asymptomatic Eye

We wondered whether, in some patients with the G11778A mutation who developed unilateral visual loss, the PERG would drop before visual loss in the fellow asymptomatic eye. We found two patients who presented with unilateral visual loss.

In the first, ETDRS acuity was 55 letters in the symptomatic right eye at study entry. It dropped to 20 letters 6 months later. In his asymptomatic left eye at baseline, ETDRS visual acuity was 71 letters (20/40, HVF MD = -0.8); however, the PERG amplitude at 0.38 μV was reduced to ~30% of normal. Six months later, visual acuity in this left eye dropped to 15 letters (~20/500, HVF MD = -22.0). Thus, the low PERG of this asymptomatic eye with good vision at baseline suggested that RGC dysfunction begins before loss of visual acuity.

The second patient lost vision in his left eye (ETDRS = three letters at baseline) with a PERG amplitude of 0.53 μV (57% of normal). His asymptomatic right eye had an ETDRS acuity of 84 letters (~20/20 at baseline, HVF MD = -2.0) and remained at 87 letters (at 6 months, HVF MD = -1.1), 82 letters (at 12 months, HVF MD = -1.5), 89 letters (at 18 months, MD = -2.2), and 88 letters (at 24 months, MD = -3.6). This right eye had

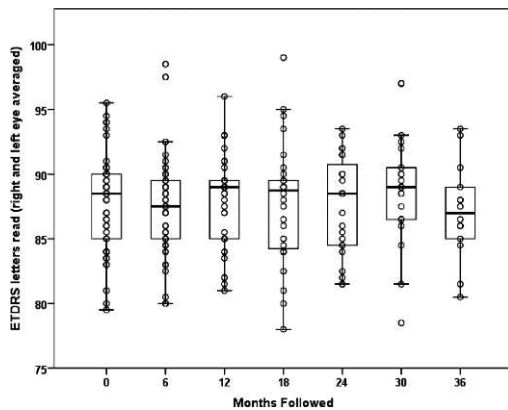


FIGURE 2. Serial visual acuity of G11778A LHON carriers from baseline to the 36-month follow-up examination.

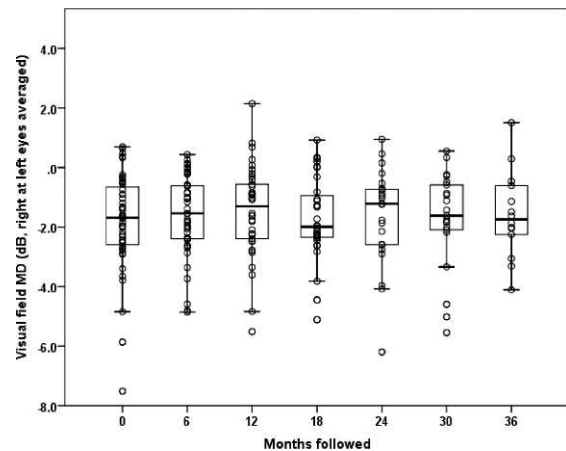


FIGURE 4. Serial visual field mean defect of G11778A LHON carriers from baseline to the 36-month follow-up examination.

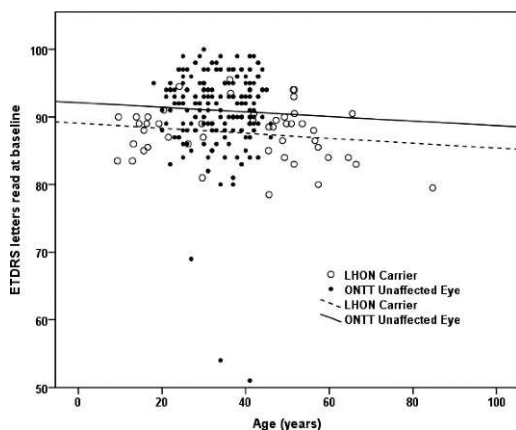


FIGURE 3. Comparisons of ETDRS visual acuity of asymptomatic ONTT fellow eyes to asymptomatic LHON carriers.

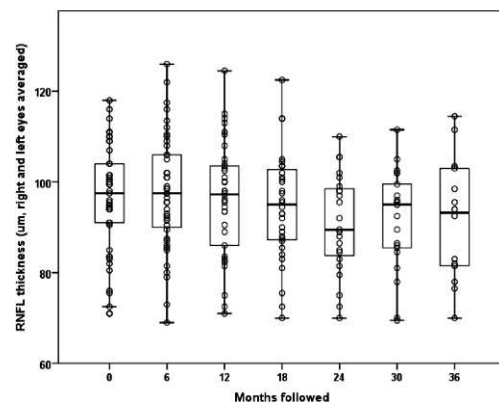


FIGURE 5. Optical coherence tomography RNFL thickness of G11778A LHON carriers from baseline to the 36-month follow-up examination.

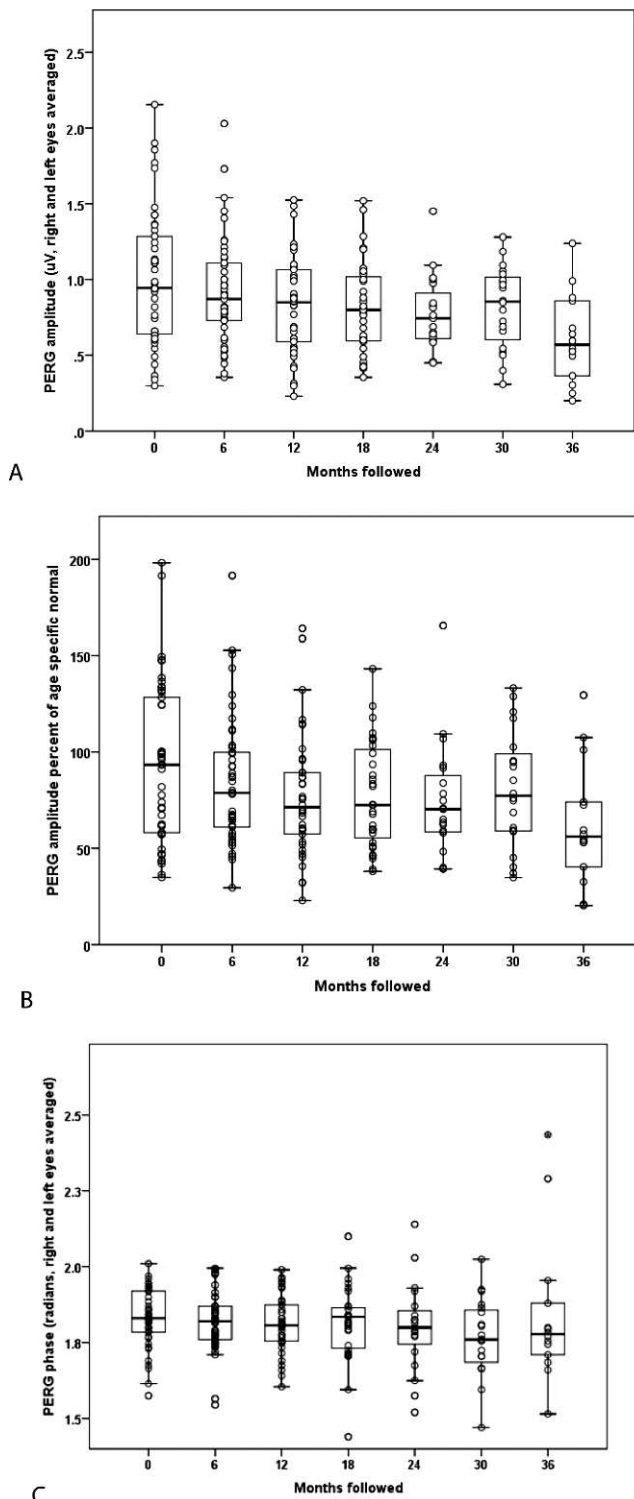


FIGURE 6. Serial PERG amplitude (A) values and relative to normal (B) and PERG phase (C) of G11778A LHON carriers from baseline to the 36-month follow-up examination.

PERG amplitudes similar to those of asymptomatic carriers with 0.76 μV at baseline that did not decline with follow-up. Despite the subtle defects on automated perimetry, the stability of the PERG in this asymptomatic eye at levels comparable to those of carriers was associated with maintenance of good visual acuity.

DISCUSSION

In the present study, we made three novel observations with respect to G11778A LHON. First, visual acuity of asymptomatic LHON carriers was slightly less than that historically observed in a young predominantly female population with a different disorder, asymptomatic fellow eyes of patients with unilateral optic neuritis in whom visual acuity was usually 20/15 to 20/10.^{27,31} In our study, we found that visual acuity was 20/20 in LHON carriers whose examinations were otherwise considered normal. For these asymptomatic G11778A LHON carriers, visual fields and OCT measurements of the RNFL did not show deterioration of statistical significance on follow-up examinations.

Second, the PERG, a sensitive measure of ganglion cell function, dropped significantly and progressively in otherwise asymptomatic G11778A subjects. This finding suggests sub-clinical ganglion cell dysfunction that is progressive. One of our carriers who had a normal PERG when asymptomatic had a more substantial decline of the PERG amplitude by approximately half when his optic disc swelled and he lost vision. It is unfortunate that for this case of conversion we had only a single baseline PERG value before visual loss for comparison. Thus, we do not know if his PERG was progressively dropping before he actually lost vision, as suggested by the mean PERG decline of our carriers over time.

Third, in one of two LHON cases who had unilateral visual loss the PERG amplitude was low in the clinically asymptomatic eye with a normal visual field and a slight drop in acuity (to 20/40) before that eye went on to develop visual loss. In the other case, with a subtle visual field defect, the PERG amplitude remained normal and this asymptomatic eye did not lose acuity. LHON is typically a bilateral disease with simultaneous onset of bilateral visual loss or visual loss in one eye first followed by visual loss in the second eye within 6 months. It is difficult to draw conclusions from only two unilateral cases, but it is intriguing that the PERG abnormality only occurred in the asymptomatic eye that later became affected. It is also intriguing that the PERG was stable in the second case that had a subtle visual field defect but he did not lose vision in the fellow eye during the 24 months of follow-up.

We have first demonstrated reductions of the PERG in asymptomatic LHON carriers.¹⁶ Those cross-sectional observations have been recently confirmed by another group.¹⁷ To our knowledge, published longitudinal data of the PERG in LHON are not available until this current study. Repeated examination of carriers (26 males, 49 females) with homoplasmic G11778A mtDNA have been performed by Sadun and coworkers^{32,33} from 2001 to 2005. They note focal nerve fiber layer swelling of the optic nerve heads in more than 20% of carriers. Most of the eyes with abnormal fundus findings also have abnormal visual fields. Of interest, the conversion rate to affected is seen in 2 of their 75 asymptomatic carriers (1.3%).

The PERG amplitude has provided a sensitive measure of ganglion cell dysfunction not only in LHON,^{17,34,35} but also in other optic nerve disorders.^{36,37} Pattern electroretinogram amplitude reductions may occur because of RGC dysfunction or loss, or a combination of both conditions. Pattern electroretinogram phase shift may occur because of latency changes of dysfunctional RGCs, because of preferential loss of RGC subpopulations that leave the PERG subserved by residual RGCs with different latency,^{38,39} or a combination of both conditions.

As we observed for LHON, progressive PERG amplitude reductions may precede the progression of visual field defects associated with glaucoma⁴⁰ or ocular hypertension by at least 1 year.⁴¹ Assuming the PERG reflects progressive RGC dysfunction or death in both LHON and glaucomatous optic

neuropathy, and that PERG progressive changes are linear in a relatively short time span, then in LHON carriers, years may pass before the PERG drops slowly to the 50% level or below seen in blind LHON patients. Whether the PERG amplitude loss predicts development of visual loss in asymptomatic eyes of those with mutated G11778A mt DNA needs further study over many more years than we were able to evaluate in this study. If it does, then perhaps these high-risk cases may be selected for more potentially robust therapeutic interventions that include gene therapy, before they experience irreversible blindness and permanent ganglion cell loss characteristic of G11778A LHON.¹¹

Acknowledgments

Supported by National Eye Institute Grants R24EY018600 (JG), RO1 EY014957 (VP), P30-EY014801 (VP), and an unrestricted grant to Bascom Palmer Eye Institute from Research to Prevent Blindness. The authors alone are responsible for the content and writing of the paper.

Disclosure: **J. Guy**, None; **W.J. Feuer**, None; **V. Porciatti**, None; **J. Schiffman**, None; **F. Abukhalil**, None; **R. Vandenbroucke**, None; **P.R. Rosa**, None; **B.L. Lam**, None

References

1. Yu-Wai-Man P, Griffiths PG, Chinnery PF. Mitochondrial optic neuropathies: disease mechanisms and therapeutic strategies. *Prog Retin Eye Res.* 2011;30:81-114.
2. Leber T. Über hereditäre und congenital-angelegete Sehnerverleiden. *Graefes Archiv für klinische und experimentelle Ophthalmologie.* 1871;7:249-271.
3. Riordan-Eva P, Sanders MD, Govan GG, et al. The clinical features of Leber's hereditary optic neuropathy defined by the presence of a pathogenic mitochondrial DNA mutation. *Brain.* 1995;118(pt 2):319-337.
4. Newman NJ, Lott MT, Wallace DC. The clinical characteristics of pedigrees of Leber's hereditary optic neuropathy with the 11778 mutation. *Am J Ophthalmol.* 1991;111:750-762.
5. Huoponen K. Leber hereditary optic neuropathy: clinical and molecular genetic findings. *Neurogenetics.* 2001;3:119-125.
6. Newman NJ, Biousse V, David R, et al. Prophylaxis for second eye involvement in leber hereditary optic neuropathy: an open-labeled, nonrandomized multicenter trial of topical brimonidine purite. *Am J Ophthalmol.* 2005;140:407-415.
7. Wallace DC, Singh G, Lott MT, et al. Mitochondrial DNA mutation associated with Leber's hereditary optic neuropathy. *Science.* 1988;242:1427-1430.
8. Guy J, Shaw G, Ross-Cisneros FN, et al. Phosphorylated neurofilament heavy chain is a marker of neurodegeneration in Leber hereditary optic neuropathy (LHON). *Mol Vis.* 2008;14:2443-2450.
9. Yee KM, Ross-Cisneros FN, Lee JG, et al. Neuron-specific enolase is elevated in asymptomatic carriers of Leber's hereditary optic neuropathy. *Invest Ophthalmol Vis Sci.* 2012;53:6389-6392.
10. Barboni P, Savini G, Feuer WJ, et al. Retinal nerve fiber layer thickness variability in Leber hereditary optic neuropathy carriers. *Eur J Ophthalmol.* 2012;22:985-991.
11. Newman NJ. Treatment of hereditary optic neuropathies. *Nat Rev Neurol.* 2012;8:545-556.
12. Klopstock T, Metz G, Yu-Wai-Man P, et al. Persistence of the treatment effect of idebenone in Leber's hereditary optic neuropathy. *Brain.* 2013;136:e230.
13. Klopstock T, Yu-Wai-Man P, Dimitriadis K, et al. A randomized placebo-controlled trial of idebenone in Leber's hereditary optic neuropathy. *Brain.* 2011;134:2677-2686.
14. Sadun AA, Chicani CF, Ross-Cisneros FN, et al. Effect of EPI-743 on the clinical course of the mitochondrial disease Leber hereditary optic neuropathy. *Arch Neurol.* 2012;69:331-338.
15. Carelli V, La MC, Valentino ML, et al. Idebenone treatment in Leber's hereditary optic neuropathy. *Brain.* 2011;134:e188.
16. Lam BL, Feuer WJ, Abukhalil F, et al. Leber hereditary optic neuropathy gene therapy clinical trial recruitment: year 1. *Arch Ophthalmol.* 2010;128:1129-1135.
17. Ziccardi L, Sadun F, De Negri AM, et al. Retinal function and neural conduction along the visual pathways in affected and unaffected carriers with Leber's hereditary optic neuropathy. *Invest Ophthalmol Vis Sci.* 2013;54:6893-6901.
18. Stone EM. Challenges in genetic testing for clinical trials of inherited and orphan retinal diseases. *Retina.* 2005;25:S72-S73.
19. Vizzeri G, Weinreb RN, Gonzalez-Garcia AO, et al. Agreement between spectral-domain and time-domain OCT for measuring RNFL thickness. *Br J Ophthalmol.* 2009;93:775-781.
20. Porciatti V, Ventura LM. Normative data for a user-friendly paradigm for pattern electroretinogram recording. *Ophthalmology.* 2004;111:161-168.
21. Fredette MJ, Anderson DR, Porciatti V, et al. Reproducibility of pattern electroretinogram in glaucoma patients with a range of severity of disease with the new glaucoma paradigm. *Ophthalmology.* 2008;115:957-963.
22. Ventura LM, Porciatti V, Ishida K, et al. Pattern electroretinogram abnormality and glaucoma. *Ophthalmology.* 2005;112:10-19.
23. Ventura LM, Golubev I, Lee W, et al. Head-down posture induces PERG alterations in early glaucoma. *J Glaucoma.* 2013;22:255-264.
24. Porciatti V, Bosse B, Parekh PK, et al. Adaptation of the steady-state PERG in early glaucoma [published online ahead of print February 19, 2013]. *J Glaucoma.*
25. Ventura LM, Sorokac N, De Los SR, et al. The relationship between retinal ganglion cell function and retinal nerve fiber thickness in early glaucoma. *Invest Ophthalmol Vis Sci.* 2006;47:3904-3911.
26. Beck RW, Cleary PA, Anderson MM Jr, et al. A randomized, controlled trial of corticosteroids in the treatment of acute optic neuritis: The Optic Neuritis Study Group. *N Engl J Med.* 1992;326:581-588.
27. Beck RW, Kupersmith MJ, Cleary PA, et al. Fellow eye abnormalities in acute unilateral optic neuritis: experience of the optic neuritis treatment trial. *Ophthalmology.* 1993;100:691-697.
28. Feuer WJ, Budenz DL, Anderson DR, et al. Topographic differences in the age-related changes in the retinal nerve fiber layer of normal eyes measured by Stratus optical coherence tomography. *J Glaucoma.* 2011;20:133-138.
29. Ventura LM, Golubev I, Feuer WJ, et al. Pattern electroretinogram progression in glaucoma suspects. *J Glaucoma.* 2013;22:219-225.
30. Fleiss JL, Kingman A. Statistical management of data in clinical research. *Crit Rev Oral Biol Med.* 1990;1:55-66.
31. The clinical profile of optic neuritis: experience of the Optic Neuritis Treatment Trial: Optic Neuritis Study Group. *Arch Ophthalmol.* 1991;109:1673-1678.
32. Sadun F, De Negri AM, Carelli V, et al. Ophthalmologic findings in a large pedigree of 11778/Haplogroup J Leber hereditary optic neuropathy. *Am J Ophthalmol.* 2004;137:271-277.
33. Sadun AA, Salomao SR, Berezovsky A, et al. Subclinical carriers and conversions in Leber hereditary optic neuropathy: a prospective psychophysical study. *Trans Am Ophthalmol Soc.* 2006;104:51-61.
34. Kurtenbach A, Leo-Kottler B, Zrenner E. Inner retinal contributions to the multifocal electroretinogram: patients

- with Leber's hereditary optic neuropathy (LHON): multifocal ERG in patients with LHON. *Doc Ophthalmol.* 2004;108:231-240.
35. Shibata K, Shibagaki Y, Nagai C, et al. Visual evoked potentials and electroretinograms in an early stage of Leber's hereditary optic neuropathy. *J Neurol.* 1999;246:847-849.
 36. Porciatti V, Ventura LM. Physiologic significance of steady-state pattern electroretinogram losses in glaucoma: clues from simulation of abnormalities in normal subjects. *J Glaucoma.* 2009;18:535-542.
 37. Ventura LM, Venzara FX III, Porciatti V. Reversible dysfunction of retinal ganglion cells in non-secreting pituitary tumors. *Doc Ophthalmol.* 2009;118:155-162.
 38. Sadun AA, Win PH, Ross-Cisneros FN, et al. Leber's hereditary optic neuropathy differentially affects smaller axons in the optic nerve. *Trans Am Ophthalmol Soc.* 2000;98:223-232.
 39. Porciatti V, Sartucci F. Retinal and cortical evoked responses to chromatic contrast stimuli: specific losses in both eyes of patients with multiple sclerosis and unilateral optic neuritis. *Brain.* 1996;119(pt 3):723-740.
 40. Bayer AU, Erb C. Short wavelength automated perimetry, frequency doubling technology perimetry, and pattern electroretinography for prediction of progressive glaucomatous standard visual field defects. *Ophthalmology.* 2002;109:1009-1017.
 41. Bach M, Unsoeld AS, Philippin H, et al. Pattern ERG as an early glaucoma indicator in ocular hypertension: a long-term, prospective study. *Invest Ophthalmol Vis Sci.* 2006;47:4881-4887.